

1      **Stable isotopic evidence for the excess leaching of unprocessed atmospheric**  
2      **nitrate from forested catchments under high nitrogen saturation**

Weitian Ding<sup>1</sup>, Urumu Tsunogai<sup>1</sup>, Fumiko Nakagawa<sup>1</sup>, Takashi Sambuichi<sup>1</sup>, Masaaki  
Chiwa<sup>2</sup>, Tamao Kasahara<sup>3</sup>, Ken'ichi Shinozuka<sup>4</sup>

<sup>1</sup>Graduate School of Environmental Studies, Nagoya University, Furo-cho, Chikusa-ku,  
Nagoya 464-8601, Japan

<sup>2</sup>Kyushu University Forest, Kyushu University

<sup>3</sup>Faculty of Agriculture, Kyushu University

<sup>4</sup>River Basin Research Center, Gifu University, 1-1 Yanagido, Gifu, 501-1193, Japan

Corresponding author: Weitian Ding

Email: ding.weitian.v2@s.mail.nagoya-u.ac.jp

3    **Abstract**

4    Owing to the elevated loading of nitrogen through atmospheric deposition, some  
5    forested ecosystems become nitrogen saturated, from which elevated levels of nitrate  
6    are exported. The average concentration of stream nitrate eluted from upstream and  
7    downstream of the Kasuya Research FK forested catchments (FK1 and FK2 catchments)  
8    in Japan were more than 90  $\mu\text{M}$ , implying that these forested catchments were under  
9    nitrogen saturation. To verify that these forested catchments were under the nitrogen  
10   saturation, we determined the export flux of unprocessed atmospheric nitrate relative to  
11   the entire deposition flux ( $M_{\text{atm}}/D_{\text{atm}}$  ratio) in these catchments, because the  $M_{\text{atm}}/D_{\text{atm}}$   
12   ratio has recently been proposed as a reliable index to evaluate nitrogen saturation in  
13   forested catchments. Specifically, we determined the temporal variation in the  
14   concentrations and stable isotopic compositions, including  $\Delta^{17}\text{O}$ , of stream nitrate in  
15   the FK catchments for more than 2 years. In addition, for comparison, the same  
16   parameters were also monitored in the Shiiba Research MY-forested catchment (MY  
17   catchment) in Japan during the same period, where the average stream nitrate  
18   concentration was low, less than 10  $\mu\text{M}$ . While showing the average nitrate  
19   concentrations of 109.5, 90.994.2, and 7.1  $\mu\text{M}$  in FK1, FK2, and MY, respectively, the  
20   catchments showed average  $\Delta^{17}\text{O}$  values of +2.6, +1.57, and +0.6 ‰ in FK1, FK2, and  
21   MY, respectively. Thus, the average concentration of unprocessed atmospheric nitrate  
22   ( $[\text{NO}_3^-_{\text{atm}}]$ ) was estimated to be 10.8, 5.16.1, and 0.2  $\mu\text{M}$  in FK1, FK2, and MY,  
23   respectively, and the  $M_{\text{atm}}/D_{\text{atm}}$  ratio was estimated to be 14.113.9, 6.67.9, and 1.32 %

24 in FK1, FK2, and MY, respectively. The estimated  $M_{atm}/D_{atm}$  ratio in FK1 ([14.1](#)[13.9](#) %)  
25 was the highest ever reported from temperate forested catchments monitored for more  
26 than 1 year. Thus, we concluded that nitrogen saturation was responsible for the  
27 enrichment of stream nitrate in the FK catchments, together with the elevated  $NO_3^-_{atm}$   
28 leaching from the catchments. While the stream nitrate concentration ( $[NO_3^-]$ ) can be  
29 affected by the amount of precipitation, the  $M_{atm}/D_{atm}$  ratio is independent of the amount  
30 of precipitation; thus, the  $M_{atm}/D_{atm}$  ratio can be used as a robust index for evaluating  
31 nitrogen saturation in forested catchments.

32

### 33 **1 Introduction**

34 Nitrate is important as a nitrogenous nutrient in the biosphere. Traditionally, forested  
35 ecosystems have been considered as nitrogen limited (Vitousek and Howarth, 1991).  
36 However, owing to the elevated loading of nitrogen through atmospheric deposition,  
37 some forested ecosystems become nitrogen saturated (Aber et al., 1989), from which  
38 elevated levels of nitrate are exported (Mitchell et al., 1997; Peterjohn et al., 1996).  
39 Such excessive leaching of nitrate from forested catchments degrades water quality and  
40 causes eutrophication in downstream areas (Galloway et al., 2003; Paerl and Huisman,  
41 2009). Thus, evaluating the stage of nitrogen saturation in each forested catchment  
42 including its temporal variation, is critical for sustainable forest management,  
43 especially for forested ecosystems under high nitrogen deposition.

44 Both concentration and seasonal variation of stream nitrate have been used as indexes

45 to evaluate the nitrogen saturation of each forested catchment in past studies (Aber,  
46 1992; Rose et al., 2015; Stoddard, 1994). A forested stream eluted from Fernow  
47 Experimental Forest USA, for instance, showed an elevated average nitrate  
48 concentration of 60  $\mu$ M, along with the absence of a seasonal variation in the stream  
49 nitrate concentration, so the forest was classified into stage 3, the highest stage of  
50 nitrogen saturation (Rose et al., 2015).

51 However, using both the concentration level (high or low) and seasonal variation  
52 (clear or absent) of stream nitrate as indexes to evaluate nitrogen saturation has  
53 limitations, including the following (1) seasonal variation of soilstream nitrate can be  
54 buffered by groundwater with in forests long residence time under humid, temperate  
55 climates such as Japan, so the, so that the seasonal variation in stream nitrate  
56 concentrations is unclear in stream nitrate concentration in Japan, even in normal forests  
57 under the nitrogen saturation stage of 0-(Mitchell et al., 1997); and (2) the stream nitrate  
58 concentration can be enriched or diluted depending on the volume of rainfall, so the  
59 concentration level can be high in low precipitation area irrespective of the stage of  
60 nitrogen saturation.

61 Nakagawa et al. (2018) lately proposed that the  $M_{atm}/D_{atm}$  ratio, the export flux of  
62 unprocessed atmospheric nitrate ( $M_{atm}$ ) relative to the deposition flux of  $NO_3^-_{atm}$  ( $D_{atm}$ ),  
63 can be an alternative, more robust index for evaluating nitrogen saturation in each  
64 forested catchment, because the  $M_{atm}/D_{atm}$  ratio directly reflects the demand for  
65 atmospheric nitrate deposited onto each forested catchments as a whole, and thus reflect

66 the nitrogen saturation in each forested catchment. That is, we can expect high  
67  $M_{atm}/D_{atm}$  ratios in forested catchments under nitrogen saturation and low  $M_{atm}/D_{atm}$   
68 ratios in forested catchments with nitrogen deficiency.

69 To estimate the  $M_{atm}/D_{atm}$  ratio accurately and precisely in each forested catchment,  
70 the fraction of unprocessed atmospheric nitrate ( $NO_3^-_{atm}$ ) in the stream needs to be  
71 estimated accurately and precisely. In recent, triple oxygen isotopic compositions of  
72 nitrate ( $\Delta^{17}O$ ) have recently been used as a conservative tracer of  $NO_3^-_{atm}$  deposited  
73 onto each forested catchment (Inoue et al., 2021; Michalski et al., 2004; Nakagawa et  
74 al., 2018; Tsunogai et al., 2014; Ding et al., 2022), showing distinctively different  $\Delta^{17}O$   
75 from that of remineralized nitrate ( $NO_3^-_{re}$ ), derived from organic nitrogen through  
76 general chemical reactions, including microbial N mineralization and microbial  
77 nitrification. While  $NO_3^-_{re}$ , the oxygen atoms of which are derived from either  
78 terrestrial  $O_2$  or  $H_2O$  through microbial processing (i.e., nitrification), always shows the  
79 relation close to the “mass-dependent” relative relation between  $^{17}O/^{16}O$  ratios and  
80  $^{18}O/^{16}O$  ratios;  $NO_3^-_{atm}$  displays an anomalous enrichment in  $^{17}O$  reflecting  
81 oxygen atom transfers from atmospheric ozone ( $O_3$ ) during the conversion of  $NO_x$  to  
82  $NO_3^-_{atm}$  (Alexander et al., 2009; Michalski et al., 2003; Morin et al., 2011; Nelson et  
83 al., 2018). As a result, the  $\Delta^{17}O$  signature defined by the following equation (Kaiser et  
84 al., 2007) enables us to distinguish  $NO_3^-_{atm}$  ( $\Delta^{17}O > 0$ ) from  $NO_3^-_{re}$  ( $\Delta^{17}O = 0$ ):

$$85 \Delta^{17}O = \frac{1 + \delta^{17}O}{(1 + \delta^{18}O)^\beta} - 1 \quad (1)$$

86 where the constant  $\beta$  is 0.5279 (Kaiser et al., 2007),  $\delta^{18}O = R_{sample}/R_{standard} - 1$  and  $R$  is

87 the  $^{18}\text{O}/^{16}\text{O}$  ratio (or the  $^{17}\text{O}/^{16}\text{O}$  ratio in the case of  $\delta^{17}\text{O}$  or the  $^{15}\text{N}/^{14}\text{N}$  ratio in the case  
88 of  $\delta^{15}\text{N}$ ) of the sample and each standard reference material. In addition,  $\Delta^{17}\text{O}$  is almost  
89 stable during “mass-dependent” isotope fractionation processes within terrestrial  
90 ecosystems. Therefore, while the  $\delta^{15}\text{N}$  or  $\delta^{18}\text{O}$  signature of  $\text{NO}_3^-_{\text{atm}}$  can be overprinted  
91 by the biological processes subsequent to deposition,  $\Delta^{17}\text{O}$  can be used as a robust tracer  
92 of unprocessed  $\text{NO}_3^-_{\text{atm}}$  to reflect its accurate mole fraction within total  $\text{NO}_3^-$ ,  
93 regardless of the progress of the partial metabolism (partial removal of nitrate through  
94 denitrification and assimilation) subsequent to deposition (Michalski et al., 2004;  
95 Nakagawa et al., 2013, 2018; Tsunogai et al., 2011, 2014, 2018).

96 Past studies reported that the maximum concentration of stream nitrate was 58.4  $\mu\text{M}$   
97 in the KJ forested catchment in Japan, with the maximum value of the  $\text{M}_{\text{atm}}/\text{D}_{\text{atm}}$  ratio  
98 was 9.4 % (Nakagawa et al., 2018; Sase et al., 2022). Whether the index of the  $\text{M}_{\text{atm}}/\text{D}_{\text{atm}}$   
99 ratio can be applied to forested catchments, where the leaching of stream nitrate is much  
100 higher than the KJ forested catchment, remained unclarified. Besides, the advantages  
101 of the  $\text{M}_{\text{atm}}/\text{D}_{\text{atm}}$  ratio within the past indexes of nitrogen saturation have not been  
102 discussed.

103 In recent, Chiwa (2021) has recently reported the enrichment of nitrate of more than  
104 90  $\mu\text{M}$  on the annual average in forested streams eluted from the FK catchments (FK1  
105 and FK2) in Kasuya Research Forest, Kyushu University, Japan (Figs. 1a and 1b). The  
106 observed enrichment of stream nitrate implied that these forested catchments were  
107 under nitrogen saturation. Thus, in this study, we determined the  $\text{M}_{\text{atm}}/\text{D}_{\text{atm}}$  ratio in the

108 FK1 and FK2 forested catchments by monitoring both the concentration and  $\Delta^{17}\text{O}$  of  
109 stream nitrate for more than 2 years to verify that these forested catchments were under  
110 nitrogen saturation. For comparison, the MY forested catchment in Shiiba Research  
111 Forest, Kyushu University, Japan (Figs. 1a and 1c), was also monitored during the same  
112 period, where the average stream nitrate concentration was low (less than 10  $\mu\text{M}$ ).  
113 Furthermore, the  $M_{\text{atm}}/D_{\text{atm}}$  ratios in these forested catchments were compared with  
114 those reported in past studies to verify the reliability of the  $M_{\text{atm}}/D_{\text{atm}}$  ratio as an index  
115 of nitrogen saturation.

116

## 117 **2 Methods**

### 118 2.1 Study sites

119 The FK forested catchments ( $33^{\circ}38'\text{N}$ ,  $130^{\circ}31'\text{E}$ ) are located in a suburban area,  
120 about 15 km west of the Fukuoka metropolitan area (the fourth largest metropolitan  
121 area in Japan). The main plantation in these catchments was Japanese cedar/cypress  
122 (Table 1). The MY forested catchment ( $32^{\circ}22'\text{N}$ ,  $131^{\circ}09'\text{E}$ ) is located in a rural area at  
123 the village of Shiiba in southern Japan's Central Kyushu Mountain range. This  
124 catchment is a mixed forest consisting of coniferous trees such as *Abies firma Sieb. et*  
125 *Zucc.*, and *Tsuga sieboldii Carr.*, and deciduous broadleaved trees such as *Quercus*  
126 *crispula Blume*, *Fagus crenata Blume*, and *Acer sieboldianum Miq.* ~~The annual average~~  
127 ~~precipitation was 1769 mm and 3837 mm at FK and MY forested catchment,~~  
128 ~~respectively, and the annual average temperature was 15.9 °C and 10.8 °C at FK and~~

129 **MY forested catchment, respectively.** Details on the studied forested catchments have

130 been described in the past studies (Chiwa, 2020, 2021).

132 **2.2 Sampling**

133 The stream water eluted from the FK1 (14 ha), FK2 (62 ha), and MY (43 ha)

134 forested catchments were collected about once every month in principle from 2019/11

135 to 2021/12 (Fig. 1). At the FK catchments, stream water was collected at upstream

136 (**FK1station A**) and downstream (**FK2station B**) locations (Fig. 1b). **At the MY**

137 **catchment, stream water was collected at station C (Fig. 1c).** Samples of stream water

138 to determine the concentration and stable isotopic compositions ( $\delta^{15}\text{N}$ ,  $\delta^{18}\text{O}$ , and  $\Delta^{17}\text{O}$ )

139 of stream nitrate were collected manually in bottles washed with deionized water before

140 sampling and then rinsed at least twice with the sample before sampling at each

141 sampling site.

142

143 **2.3 Analysis**

144 All the stream water samples were passed through a membrane filter (pore size 0.45

145  $\mu\text{m}$ ) within two days after sampling and stored in a refrigerator (4 °C) until

146 analysis. The concentrations of nitrate were measured by ion chromatography

147 (Prominence HIC-SP, Shimadzu, Japan). To determine the stable isotopic compositions

148 of nitrate in the stream water samples, nitrate in each sample was chemically converted

149 to  $\text{N}_2\text{O}$  using a method originally developed to determine the  $^{15}\text{N}/^{14}\text{N}$  and  $^{18}\text{O}/^{16}\text{O}$  ratios

150 of seawater and freshwater nitrate (McIlvin and Altabet, 2005) that was later modified  
151 (Konno et al., 2010; Tsunogai et al., 2011; Yamazaki et al., 2011). In brief, 11 mL of  
152 each sample solution was pipetted into a vial with a septum cap. Then, 0.5 g of spongy  
153 cadmium was added, followed by 150  $\mu$ L of a 1 M NaHCO<sub>3</sub> solution. The sample was  
154 then shaken for 18-24 h at a rate of 2 cycles s<sup>-1</sup>. Then, the sample solution (10 mL) was  
155 decanted into a different vial with a septum cap. After purging the solution using high-  
156 purity helium, 0.4 mL of an azide-acetic acid buffer, which had also been purged using  
157 high-purity helium, was added. After 45 min, the solution was alkalinized by adding  
158 0.2 mL of 6 M NaOH. Then, the stable isotopic compositions ( $\delta^{15}\text{N}$ ,  $\delta^{18}\text{O}$ , and  $\Delta^{17}\text{O}$ ) of  
159 the N<sub>2</sub>O in each vial were determined using the continuous-flow isotope ratio mass  
160 spectrometry (CF-IRMS) system at Nagoya University. The analytical procedures  
161 performed using the CF-IRMS system were the same as those detailed in previous  
162 studies (Hirota et al., 2010; Komatsu et al., 2008a). The obtained values of  $\delta^{15}\text{N}$ ,  $\delta^{18}\text{O}$ ,  
163 and  $\Delta^{17}\text{O}$  for the N<sub>2</sub>O derived from the nitrate in each sample were compared with those  
164 derived from our local laboratory nitrate standards to calibrate the values of the sample  
165 nitrate to an international scale and to correct for both isotope fractionation during the  
166 chemical conversion to N<sub>2</sub>O and the progress of oxygen isotope exchange between the  
167 nitrate derived reaction intermediate and water (ca. 20 %). ~~The local laboratory nitrate~~  
168 ~~standards used for the calibration had been calibrated using the internationally~~  
169 ~~distributed isotope reference materials (USGS 34 and USGS 35)~~. In this study, we  
170 adopted the internal standard method to calibrate the stable isotopic compositions of

171 sample nitrate (Ding et al., 2022; Nakagawa et al., 2013, 2018; Tsunogai et al., 2014).  
172

172 Specifically, three kinds of the local laboratory nitrate standards were used in this study,  
173 which were named to be GG01 ( $\delta^{15}\text{N} = -3.07 \text{ ‰}$ ,  $\delta^{18}\text{O} = +1.10 \text{ ‰}$ , and  $\Delta^{17}\text{O} = 0 \text{ ‰}$ ),  
174 HDLW02 ( $\delta^{15}\text{N} = +8.94 \text{ ‰}$ ,  $\delta^{18}\text{O} = +24.07 \text{ ‰}$ ), and NF ( $\Delta^{17}\text{O} = +19.16 \text{ ‰}$ ), which the  
175 GG01 and the HDLW02 were used to determine the  $\delta^{15}\text{N}$  and  $\delta^{18}\text{O}$  of stream nitrate,  
176 and the GG01 and the NF was used to determine the  $\Delta^{17}\text{O}$  of stream nitrate. The GG01,  
177 HDLW02, and NF had been calibrated using the internationally distributed isotope  
178 reference materials (USGS 34 and USGS 35). The oxygen exchange rate between  
179 nitrate and water during the chemical conversion was calculated through Eq. (2):

180 Oxygen exchange rate (%) =  $\Delta^{17}\text{O}(\text{N}_2\text{O})_{\text{NF}} / \Delta^{17}\text{O}(\text{NO}_3^-)_{\text{NF}}$  (2)

181 where the  $\Delta^{17}\text{O}(\text{N}_2\text{O})_{\text{NF}}$  denote the  $\Delta^{17}\text{O}$  value of  $\text{N}_2\text{O}$  that convert from the NF  
182 nitrate, the  $\Delta^{17}\text{O}(\text{NO}_3^-)_{\text{NF}}$  denote the  $\Delta^{17}\text{O}$  value of NF nitrate ( $\Delta^{17}\text{O} = +19.16 \text{ ‰}$ )  
183 (Tsunogai et al., 2016; Nakagawa et al., 2013, 2018; Ding et al., 2022).

184 The  $\delta^2\text{H}$  and  $\delta^{18}\text{O}$  values of  $\text{H}_2\text{O}$  of the stream water samples were analyzed using  
185 the cavity ring-down spectroscopy method by employing an L2120-i instrument  
186 (Picarro Inc., Santa Clara, CA, USA) equipped with an A0211 vaporizer and  
187 autosampler. The errors (standard errors of the mean) in this method were  $\pm 0.5\text{ ‰}$  for  
188  $\delta^2\text{H}$  and  $\pm 0.1\text{ ‰}$  for  $\delta^{18}\text{O}$ . Both the VSMOW and standard light Antarctic precipitation  
189 (SLAP) were used to calibrate the values to the international scale. The  $\delta^{18}\text{O}$  values of  
190  $\text{H}_2\text{O}$  were used to calibrate the differences in  $\delta^{18}\text{O}$  of  $\text{H}_2\text{O}$  between the samples and  
191 those our local laboratory nitrate standard samples (Tsunogai et al., 2010, 2011, 2014).

192 To determine whether the conversion rate from nitrate to N<sub>2</sub>O was sufficient, the  
193 concentration of nitrate in the samples was determined each time we analyzed the  
194 isotopic composition using CF-IRMS based on the N<sub>2</sub>O<sup>+</sup> or O<sub>2</sub><sup>+</sup> outputs. We adopted  
195 the δ<sup>15</sup>N, δ<sup>18</sup>O, and Δ<sup>17</sup>O values only when the concentration measured via CF-IRMS  
196 correlated with the concentration measured via ion chromatography prior to isotope  
197 analysis within a difference of 10 %. We repeated the analysis of δ<sup>15</sup>N, δ<sup>18</sup>O, and Δ<sup>17</sup>O  
198 values for each sample at least three times to attain high precision. All samples had a  
199 nitrate concentration of greater than 3.5 μM, which corresponded to a nitrate quantity  
200 greater than 35 nmol in a 10 mL sample. Thus, all isotope values presented in this study  
201 have an error (standard error of the mean) better than ±0.2 ‰ for δ<sup>15</sup>N, ±0.3 ‰ for δ<sup>18</sup>O,  
202 and ±0.1 ‰ for Δ<sup>17</sup>O.

203 Nitrite (NO<sub>2</sub><sup>−</sup>) in the samples interferes with the final N<sub>2</sub>O produced from nitrate  
204 because the chemical method also converts NO<sub>2</sub><sup>−</sup> to N<sub>2</sub>O (McIlvin and Altabet, 2005).  
205 Therefore, it is sometimes necessary to remove NO<sub>2</sub><sup>−</sup> prior to converting nitrate to N<sub>2</sub>O.  
206 In this study, however, we skipped the processes for removing NO<sub>2</sub><sup>−</sup> because all the  
207 stream samples analyzed for stable isotopic composition had NO<sub>2</sub><sup>−</sup> concentrations lower  
208 than the detection limit (0.05 μM).

209  
210 2.4 Deposition rate of atmospheric nitrate

211 The annual deposition rate of atmospheric nitrate (D<sub>atm</sub>; total dry and wet deposition  
212 rate of atmospheric nitrate) in each catchment was estimated using the annual “bulk”

213 deposition rate of atmospheric nitrate ( $D_{bulk}$ ) calculated in Chiwa (2020) at each  
214 catchment by multiplying the volume-weighted mean concentration of nitrate in the  
215 bulk deposition samples collected every 2 weeks at each catchment for 10 years (from  
216 2009/1 to 2018/12) by the annual amount of precipitation. The bulk deposition samples  
217 were ~~samples those~~ accumulated in a plastic bucket installed in an open site of each  
218 catchment 55 cm above the ground. ~~The concentrations of nitrate in these samples were~~  
219 ~~measured by ion chromatography. The distances between the monitoring sites of bulk~~  
220 ~~deposition in the FK1, FK2, and MY forested catchments and the stations of stream~~  
221 ~~water sampling (stations A, B, and C) were 3.9, 2.9, and 4.5 km, respectively. The~~  
222 ~~concentrations of nitrate in the bulk deposition samples were measured by ion~~  
223 ~~chromatography.~~

224 The  $D_{bulk}$  determined through this method, however, is less than  $D_{atm}$  (Aikawa et al.,  
225 2003) because the dry deposition velocities of gases and particles on the water surface  
226 of the plastic bucket are smaller than those on the forest (Matsuda, 2008). Thus, we  
227 corrected the differences by using Eq. (32) to estimate  $D_{atm}$  from  $D_{bulk}$ :

$$D_{atm} = D_{bulk} - D_{dry}(W) + D_{dry}(F) \quad (32)$$

228 where  $D_{dry}(W)$  and  $D_{dry}(F)$  denote the annual dry deposition rates onto water and forest,  
229 respectively.

230 The  $D_{dry}(W)$  and  $D_{dry}(F)$  at each catchment were determined using an inferential  
231 method (Endo et al., 2011) through Eqs. (43) and (54), respectively:

$$D_{dry}(W) = [NO_3^-]_{atm} \times V_{gas}(W) + [NO_3^-]_p \times V_p(W) \quad (43)$$

234  $D_{dry}(F) = [NO_3^-]_{atm, gas} \times V_{gas}(F) + [NO_3^-]_p \times V_p(F)$  (54)

235 where  $[NO_3^-]_{atm, gas}$  denotes the concentration of gaseous nitrate in air;  $[NO_3^-]_p$   
236 denotes the concentration of particle nitrate in air;  $V_{gas}(W)$  and  $V_{gas}(F)$  denote the  
237 deposition velocities of gaseous nitrate on the water surface and forest, respectively;  
238 and  $V_p(W)$  and  $V_p(F)$  denote the deposition velocities of particulate nitrate on the water  
239 surface and forest, respectively. Those determined by Chiwa (2010) using the annular  
240 denuder method from 2006/5 to 2007/4 were used for the  $[NO_3^-]_{gas}$  and  $[NO_3^-]_p$  in the  
241 FK catchments. Those determined by the National Institute for Environmental Studies  
242 (Environmental Laboratories Association of Japan, 2017) using the filter-pack method  
243 at Miyazaki (31°83'N, 131°42'E) from 2011 to 2017 were used for the  $[NO_3^-]_{gas}$  and  
244  $[NO_3^-]_p$  in the MY catchment. The  $V_{gas}(F)$ ,  $V_{gas}(W)$ ,  $V_p(F)$ , and  $V_p(W)$  of each  
245 catchment were determined by applying the estimation file for dry deposition (Matsuda,  
246 2008;

247 [http://www.hro.or.jp/list/environmental/research/ies/katsudo/acid\\_rain/kanseichinchaku](http://www.hro.or.jp/list/environmental/research/ies/katsudo/acid_rain/kanseichinchaku)  
248 u/kanseichinchaku.html), where  $V_{gas}$  and  $V_p$  were calculated using the meteorological  
249 data of wind speed, temperature, humidity, radiation, and cloud amount and land use.

250 The meteorological data monitored by Japan Meteorological Agency at the nearest  
251 Fukuoka station (33°34'N, 130°22'E) and Miyazaki station (31°56'N, 131°24'E) from  
252 2009 to 2021<sup>18</sup> were used for the FK and MY catchments, respectively. The forested  
253 land use of 100 % was chosen for each area.

254

255 2.5 Flux of stream water

256 The flux of stream water ( $F_{\text{stream}}$ ) in each catchment was not measured directly fully  
257 in this study. Instead, the water balance in each catchment was used to estimate  $F_{\text{stream}}$ ,  
258 assuming that the outflux of water from the study catchments to deep groundwater was  
259 negligible:

260  $F_{\text{stream}} = P - E$  (65)

261 where  $P$  denotes the annual average precipitation and  $E$  denotes the annual  
262 evapotranspiration flux of water in each catchment. In this paper, the equation obtained  
263 by Komatsu et al. (2008) was used to estimate the  $E$  of the FK and MY catchments.

264 Details on this equation are shown below.

265 Komatsu et al. (2008) compiled the annual flux of evapotranspiration determined in  
266 43 forested catchments in Japan and found that  $E$  shows a positive correlation with the  
267 average temperature ( $T_{\text{avg}}$ ) of each catchment. Thus, they proposed the modeled relation  
268 of  $E$  (mm) =  $31.4T_{\text{avg}}$  ( $^{\circ}\text{C}$ ) + 376 to estimate  $E$  in each forested catchment in Japan,  
269 where the standard error of 162.3 mm was included in the estimated evapotranspiration  
270 flux (E).

271

272 2.6 Concentration of unprocessed  $\text{NO}_3^-_{\text{atm}}$  in each water sample

273 The  $\Delta^{17}\text{O}$  data of nitrate in each sample was used to estimate the concentration of  
274  $\text{NO}_3^-_{\text{atm}}$  ( $[\text{NO}_3^-_{\text{atm}}]$ ) in each water sample by applying Eq. (76):

275  $[\text{NO}_3^-_{\text{atm}}]/[\text{NO}_3^-] = \Delta^{17}\text{O}/\Delta^{17}\text{O}_{\text{atm}}$  (76)

276 where  $[\text{NO}_3^-_{\text{atm}}]$  and  $[\text{NO}_3^-]$  denote the concentrations of  $\text{NO}_3^-_{\text{atm}}$  and nitrate (total) in  
277 each water sample, respectively, and  $\Delta^{17}\text{O}_{\text{atm}}$  and  $\Delta^{17}\text{O}$  denote the  $\Delta^{17}\text{O}$  values of  
278  $\text{NO}_3^-_{\text{atm}}$  and nitrate (total) in the stream water sample, respectively. In this study, we  
279 used the annual average  $\Delta^{17}\text{O}$  value of  $\text{NO}_3^-_{\text{atm}}$  determined at the Sado-Seki monitoring  
280 station in Japan (Sado Island; Fig. 1a) from April 2009 to March 2012 ( $\Delta^{17}\text{O}_{\text{atm}} =$   
281  $+26.3\text{ ‰}$ ; Tsunogai et al., 2016) for  $\Delta^{17}\text{O}_{\text{atm}}$  in Eq. (72) to estimate  $[\text{NO}_3^-_{\text{atm}}]$  in the  
282 stream. We allow for an error range of 3 ‰ in  $\Delta^{17}\text{O}_{\text{atm}}$ , where the factor changes in  
283  $\Delta^{17}\text{O}_{\text{atm}}$  from  $+26.3\text{ ‰}$  caused by both areal and seasonal variations in the  $\Delta^{17}\text{O}$  values  
284 of  $\text{NO}_3^-_{\text{atm}}$  have been considered (Nakagawa et al., 2018; Tsunogai et al., 2016; Ding et  
285 al., 2022).

286 The annual export flux of unprocessed  $\text{NO}_3^-_{\text{atm}}$  per unit area of the catchment ( $M_{\text{atm}}$ )  
287 was determined by applying Eq. (87):

$$288 M_{\text{atm}} = [\text{NO}_3^-_{\text{atm}}]_{\text{avg}} \times F_{\text{stream}} \quad (87)$$

289 where  $[\text{NO}_3^-_{\text{atm}}]_{\text{avg}}$  denotes the annual average  $[\text{NO}_3^-_{\text{atm}}]$  in each stream. The index of  
290 nitrogen saturation ( $M_{\text{atm}}/D_{\text{atm}}$  ratio) was calculated by dividing  $M_{\text{atm}}$  with  $D_{\text{atm}}$  in each  
291 catchment.

292  
293 2.7 Concentration and isotopic compositions of stream nitrate eluted only from the FK2  
294 catchment

295 The concentration and isotopic compositions ( $\delta^{15}\text{N}$ ,  $\delta^{18}\text{O}$ , and  $\Delta^{17}\text{O}$ ) of stream nitrate  
296 determined at the station B were the mixture of those eluted from FK1 and FK2

297 catchments (Fig. 1b). Assuming that the stream nitrate eluted from FK1 catchment was  
298 stable during the flow path from station A to station B. The concentration of stream  
299 nitrate eluted from the FK2 catchment was determined by applying Eq. (9):

300 
$$[\text{NO}_3^-]_{\text{FK2}} = ([\text{NO}_3^-]_{\text{FK1+FK2}} * F_{\text{FK1+FK2}} - [\text{NO}_3^-]_{\text{FK1}} * F_{\text{FK1}}) / F_{\text{FK2}} \quad (9)$$

301 where  $F_{\text{FK1}}$ ,  $F_{\text{FK2}}$ , and  $F_{\text{FK1+FK2}}$  denote the flux of stream water eluted from the FK1,  
302 FK2 (only), and FK1+FK2 catchment, respectively.  $[\text{NO}_3^-]_{\text{FK1}}$ ,  $[\text{NO}_3^-]_{\text{FK2}}$ , and  
303  $[\text{NO}_3^-]_{\text{FK1+FK2}}$  denote the concentration of stream nitrate eluted from the FK1, FK2  
304 (only), and FK1+FK2 catchment, respectively. In this study, the flow rates measured at

305 stations A and B on 2021/01/15 by using the salt dilution method (Sappa et al., 2015)

306 was used for  $F_{\text{FK1}}$  (0.85 L/s) and  $F_{\text{FK1+FK2}}$  (4.75 L/s), respectively, and the measured

307  $[\text{NO}_3^-]$  at stations A and B was used for  $[\text{NO}_3^-]_{\text{FK1}}$  and  $[\text{NO}_3^-]_{\text{FK1+FK2}}$ , respectively.

308 Because the relation between the measured flow rates was comparable with the relation

309 between the catchment area of FK1 (14 ha) and that of FK1+FK2 (76 ha), we concluded

310 that the measured flow rates of 0.85 L/s and 4.75 L/s were reasonable as for those

311 representing the  $F_{\text{FK1}}$  and  $F_{\text{FK1+FK2}}$ , respectively. According to the mass balance of water,

312 we can estimate the  $F_{\text{FK2}}$  eluted from the FK2 catchment only to be 3.90 L/s.

313 Assuming that the stream nitrate eluted from FK1 catchment was stable during the

314 flow path from station A to station B, the  $\delta^{15}\text{N}$ ,  $\delta^{18}\text{O}$ , and  $\Delta^{17}\text{O}$  values of stream nitrate

315 eluted from the FK2 catchment only were determined by applying Eq. (10):

316 
$$\delta_{\text{FK2}} = (\delta_{\text{FK1+FK2}} * [\text{NO}_3^-]_{\text{FK1+FK2}} * F_{\text{FK1+FK2}} - \delta_{\text{FK1}} * [\text{NO}_3^-]_{\text{FK1}} * F_{\text{FK1}}) / ([\text{NO}_3^-]_{\text{FK2}} * \quad (10)$$

317  $F_{\text{FK2}})$

318 where  $\delta_{FK1}$ ,  $\delta_{FK2}$ , and  $\delta_{FK1+FK2}$  denote the  $\delta^{15}\text{N}$  (or  $\delta^{18}\text{O}$  or  $\Delta^{17}\text{O}$ ) of stream nitrate eluted  
319 from the FK1, FK2, and FK1+FK2 catchment, respectively. The  $\delta^{15}\text{N}$  (or  $\delta^{18}\text{O}$  or  $\Delta^{17}\text{O}$ )  
320 values of stream nitrate measured at stations A and B were used for  $\delta_{FK1}$  and  $\delta_{FK1+FK2}$ ,  
321 respectively.

322

### 323 3 Results

#### 324 3.1 Deposition rate of atmospheric nitrate

325 The mean annual precipitation (P) from 2009 to 2021 was 1777 mm and 3981 mm  
326 for FK and MY catchments, respectively (Chiwa, 2020; Chiwa, personal  
327 communication, September 21, 2022). The mean annual temperature ( $T_{avg}$ ) was  
328 reported to be 15.9 °C and 10.8 °C for FK and MY catchments, respectively (Chiwa,  
329 2020). Chiwa (2020) estimated the mean annual precipitation (P) and mean annual  
330 temperature ( $T_{avg}$ ) to be 1769 mm and 15.9 °C, respectively, at FK catchments, and  
331 3837 mm and 10.8 °C, respectively, at MY catchment. Based on these data, the annual  
332 flux of stream water ( $F_{stream}$ ) was estimated to be 902.0893.7  $\pm$  162.3 mm at FK  
333 catchments and 3266.13121.9  $\pm$  162.3 mm at MY catchment, respectively, using Eq.  
334 (65), corresponding to  $1.25 \times 10^5 \text{ m}^3/\text{year}$  in FK1,  $5.54 \times 10^5 \text{ m}^3/\text{year}$  in FK2, and  $1.34$   
335  $\times 10^6 \text{ m}^3/\text{year}$  in MY.

336 Chiwa (2020) also reported the annual bulk deposition rates of atmospheric nitrate  
337 ( $D_{bulk}$ ) to be 34.0  $\text{mmol m}^{-2} \text{ year}^{-1}$  at FK catchments and 24.2  $\text{mmol m}^{-2} \text{ year}^{-1}$  at MY  
338 catchment. On the other hand, the annual dry deposition rate of atmospheric nitrate

339 ( $D_{dry}$ ) deposited ~~on~~in the forest ( $D_{dry}(F)$ ) and on the water surface ( $D_{dry}(W)$ ) were  
340 estimated to be 39.98 mmol m<sup>-2</sup> year<sup>-1</sup> and 4.1 mmol m<sup>-2</sup> year<sup>-1</sup>, respectively, at FK  
341 catchments, and 18.4 mmol m<sup>-2</sup> year<sup>-1</sup> and 2.4 mmol m<sup>-2</sup> year<sup>-1</sup>, respectively, at MY  
342 catchment. As a result,  $D_{atm}$  was estimated to be 69.3 mmol m<sup>-2</sup> year<sup>-1</sup> at FK catchments  
343 and 40.1 mmol m<sup>-2</sup> year<sup>-1</sup> at MY catchments, using Eq. (32).

344

### 345 3.2 Concentration and isotopic composition of stream nitrate

346 The concentrations of stream nitrate ~~at eluted from~~ the FK1, FK2 (only), and MY  
347 catchments ranged from 97.5  $\mu$ M to 121.3  $\mu$ M, from 73.9~~65.7~~  $\mu$ M to 148.5~~142.6~~  $\mu$ M,  
348 and from 3.5  $\mu$ M to 15.3  $\mu$ M, respectively, with the average concentrations of 109.5  
349  $\mu$ M, 90.9~~94.2~~  $\mu$ M, and 7.3  $\mu$ M, respectively, and the standard deviations (SD) of 6.3  
350  $\mu$ M, 18.5  $\mu$ M, and 3.0  $\mu$ M, respectively, which corresponds to the coefficients of  
351 variation (CV) of 5.7 %, 20.4 %, and 40.7 %, respectively (Fig. 2a). All catchments  
352 showed ~~no clear~~little seasonal variation during the observation periods. The variation  
353 ranges and the average concentrations of stream nitrate ~~in eluted from~~ the three  
354 catchments agreed well with the past observations performed in the same catchments  
355 (Chiwa, 2021).—

356 The stable isotopic compositions of stream nitrate ~~at eluted from~~ the FK1, FK2 (only),  
357 and MY catchments ranged from -0.9 ‰ to +1.5 ‰, from -1.4~~2~~ ‰ to +5.8~~4.5~~ ‰, and  
358 from -0.8 ‰ to +2.4 ‰, respectively, for  $\delta^{15}\text{N}$  (Fig. 2b), from +3.9 ‰ to +8.5 ‰, from  
359 -0.7~~2.2~~ ‰ to +2.8~~3.6~~ ‰, and from -5.6 ‰ to +1.7 ‰, respectively, for  $\delta^{18}\text{O}$  (Fig. 2c),

360 and from +2.0 ‰ to +3.3 ‰, from +0.68 ‰ to +2.24 ‰, and from +0.2 ‰ to +1.0 ‰,  
361 respectively, for  $\Delta^{17}\text{O}$  (Fig. 2d), with ~~little~~ ~~no~~ ~~clear~~ seasonal variation during the  
362 observation periods. The concentration-weighted averages for the  $\delta^{15}\text{N}$ ,  $\delta^{18}\text{O}$ , and  $\Delta^{17}\text{O}$   
363 values of stream nitrate were +0.2 ‰, +6.4 ‰, and +2.6 ‰, respectively, at FK1,  
364 +1.00.9 ‰, +0.51.7 ‰, and +1.51.7 ‰, respectively, at FK2, +0.7 ‰, -2.5 ‰, and  
365 +0.6 ‰, respectively, at MY. ~~These values were typical for stream nitrate eluted from~~  
366 ~~forested catchments (Hattori et al., 2019; Huang et al., 2020; Nakagawa et al., 2013,~~  
367 ~~2018; Riha et al., 2014; Sabo et al., 2016; Tsunogai et al., 2014, 2016).~~

368

369 3.3 Concentration of unprocessed atmospheric nitrate and the  $\text{M}_{\text{atm}}/\text{D}_{\text{atm}}$  ratio in each  
370 catchment

371 The concentration of unprocessed atmospheric nitrate ( $[\text{NO}_3^-]_{\text{atm}}$ ) in the streams ~~of~~  
372 ~~eluted from~~ the FK1, FK2 ~~(only)~~, and MY catchments ranged from 8.64 to 14.30  $\mu\text{M}$ ,  
373 from 3.88~~2.27~~ to 11.16~~10.71~~  $\mu\text{M}$ , and from 0.03 to 0.46  $\mu\text{M}$  with the average  
374 concentration of  $10.80 \pm 1.65$ , ~~6.09~~5.06  $\pm$  ~~1.05~~0.92, and  $0.16 \pm 0.05 \mu\text{M}$ , respectively,  
375 even though these ~~studied~~ catchments showed little seasonal variations during the  
376 observation periods (Fig. 2e). The annual export flux of nitrate ( $\text{M}_{\text{total}}$ ), the annual  
377 export flux of  $\text{NO}_3^-$  ( $\text{M}_{\text{atm}}$ ), and the  $\text{M}_{\text{atm}}/\text{D}_{\text{atm}}$  ratio were ~~98.8~~97.9  $\pm$  17.8  $\text{mmol m}^{-2}$   
378  $\text{year}^{-1}$ ,  $9.7 \pm 2.3 \text{ mmol m}^{-2} \text{ year}^{-1}$ , and ~~14.1~~13.9  $\pm$  4.43 % at FK1 catchment,  
379 respectively, ~~84.2~~82.0  $\pm$  ~~15.3~~14.8  $\text{mmol m}^{-2} \text{ year}^{-1}$ , ~~5.4~~4.6  $\pm$  1.24  $\text{mmol m}^{-2} \text{ year}^{-1}$ , and  
380 ~~6.6~~7.9  $\pm$  2.15 % at FK2 catchment, respectively, ~~23.7~~22.6  $\pm$  1.2  $\text{mmol m}^{-2} \text{ year}^{-1}$ ,  $0.5 \pm$

381 0.24 mmol m<sup>-2</sup> year<sup>-1</sup>, and 1.32 ± 0.54 % at MY catchment, respectively (Table 2).

382

383 **4 Discussion**

384 **4.1 Deposition rate of atmospheric nitrate at the study catchments**

385 Based on the air monitoring data determined at the stations of Fukuoka (33°51'N,

386 130°50'E) and Miyazaki (31°83'N, 131°42'E) from 2011 to 2017, the Environmental

387 Laboratories Association of Japan (2017) reported  $D_{atm}$  to be 57.8 mmol m<sup>-2</sup> year<sup>-1</sup> at

388 Fukuoka and 49.1 mmol m<sup>-2</sup> year<sup>-1</sup> at Miyazaki. Those values are consistent with the

389  $D_{atm}$  estimated in this study (69.3 and 40.1 mmol m<sup>-2</sup> year<sup>-1</sup> at the FK and MY

390 catchments, respectively), within a difference of approximately 20 %. Thus, we

391 concluded that the  $D_{atm}$  estimated in this study was reliable within the error margin of

392 20 % (Table 2). Because the  $D_{atm}$  determined at the FK catchments was the highest

393 among the forested catchments in Table 3, we further compared the  $D_{atm}$  of the FK

394 catchments with those from the other air monitoring stations in Japan reported in past

395 studies, along with that of the MY catchment (Table S1). While the  $D_{atm}$  of the MY

396 catchment corresponded to the average level among the sites compiled in Table S1, the

397  $D_{atm}$  of the FK catchments exceeded the average level significantly. In addition, the  $D_{atm}$

398 of the FK catchments corresponded to one of the highest among the Japanese forested

399 areas (Table S1). While a All the catchments in Japan this study can be suffered from the

400 long-range transport of air pollutants derived from megacities in East Asian region

401 (Chiwa, 2021; Chiwa et al., 2012 and 2013). In addition, the shorter transport distance

402 from the Fukuoka metropolitan area (total population: 1.62 million people; population  
403 density: 4715 people/km<sup>2</sup>) may be mainly responsible for the D<sub>atm</sub> higher in FK than in  
404 MY, because the FK catchments are only 15 km west of the Fukuoka metropolitan area.  
405 ~~As a result, the local emission in the Fukuoka metropolitan area should be responsible~~  
406 ~~for the high D<sub>atm</sub> at the FK catchments.~~

407

408 4.2 Excess leaching of unprocessed atmospheric nitrate from FK catchments

409 The isotopic compositions ( $\delta^{15}\text{N}$ ,  $\delta^{18}\text{O}$ , and  $\Delta^{17}\text{O}$ ) of stream nitrate eluted from the  
410 FK and MY catchments were typical for those eluted from forested catchments (Hattori  
411 et al., 2019; Huang et al., 2020; Nakagawa et al., 2013, 2018; Riha et al., 2014; Sabo et  
412 al., 2016; Tsunogai et al., 2014, 2016). The striking features found in the FK catchments  
413 were that, in addition to the high [NO<sub>3</sub><sup>-</sup>] and high M<sub>total</sub> that had been clarified prior to  
414 this in a past study (Chiwa, 2021), both [NO<sub>3</sub><sup>-</sup><sub>atm</sub>] and M<sub>atm</sub> in FK were higher than those  
415 in eluted from MY (Table 2). Especially, the average [NO<sub>3</sub><sup>-</sup><sub>atm</sub>] in the stream eluted in  
416 the from the FK1 stream catchment was the highest ever reported in forested streams  
417 determined through continuous monitoring for more than 1 year (Bostic et al., 2021;  
418 Bourgeois et al., 2018b, 2018a; Hattori et al., 2019; Huang et al., 2020; Nakagawa et  
419 al., 2018; Rose et al., 2015; Sabo et al., 2016; Tsunogai et al., 2014, 2016).

420 The observed high [NO<sub>3</sub><sup>-</sup><sub>atm</sub>] in the FK1 stream eluted from the FK1 catchment could  
421 be caused just by the high [NO<sub>3</sub><sup>-</sup><sub>atm</sub>] in deposition in the catchment D<sub>atm</sub>. Thus, we  
422 compiled all past data ever reported in forested streams through continuous monitoring

423 in Table 3, where the data of average  $[\text{NO}_3^-]$ , average  $[\text{NO}_3^-_{\text{atm}}]$ ,  $M_{\text{atm}}$ ,  $M_{\text{total}}$ ,  $D_{\text{atm}}$ , and  
424  $M_{\text{atm}}/D_{\text{atm}}$  ratio were included for comparison.~~5 and t~~The result showed that the FK  
425 ~~catchment has the highest~~ $M_{\text{atm}}/D_{\text{atm}}$  ratio, along with~~M~~ $M_{\text{atm}}$ , ~~was the highest as well in~~  
426 ~~the FK1 catchment~~ among the forested catchments (Table 3).

427 Elevated loading of nitrogen through atmospheric deposition was responsible for the  
428 occurrence of nitrogen saturation in forest ecosystems, from which elevated levels of  
429 nitrate are exported (Aber et al., 1989). Nakagawa et al. (2018) proposed that the  
430  $M_{\text{atm}}/D_{\text{atm}}$  ratio can be an index for evaluating the nitrogen saturation in each forested  
431 catchment, because the  $M_{\text{atm}}/D_{\text{atm}}$  ratio directly reflects the present demand for  
432 atmospheric nitrate deposited in each forested catchment, and thus reflects the nitrogen  
433 saturation in each forested catchment. The high  $M_{\text{atm}}/D_{\text{atm}}$  ratios observed in the FK  
434 catchments implied that ~~the demand for atmospheric nitrate was low in the FK~~  
435 ~~catchments and~~ ~~the~~ stages of nitrogen saturation at the FK catchments were  
436 higher than those at other forested catchments.~~5 and thus~~That is, the nitrogen saturation  
437 at the FK catchments was responsible for the observed higher ~~observed~~  $[\text{NO}_3^-]$  and high  
438  $M_{\text{total}}$  at the FK catchments than at MY and any other catchment ever studied (Table 3).

439 The stand age of forests can affect the retention or loss of N (Fukushima et al., 2011;  
440 Ohrui and Mitchell, 1997). Fukushima et al. (2011) evaluated N uptake rates of  
441 Japanese cedars at different ages (5-89 years old) and demonstrated that the N uptake  
442 rates of Japanese cedars were higher in younger stands ( $53 \text{ kg N ha}^{-1} \text{ year}^{-1}$  in 16 years  
443 old) than in older stands ( $29 \text{ kg N ha}^{-1} \text{ year}^{-1}$  in 31 years old;  $24 \text{ kg N ha}^{-1} \text{ year}^{-1}$  in 42

444 years old;  $34 \text{ kg N ha}^{-1} \text{ year}^{-1}$  in 89 years old). In addition, Yang and Chiwa (2021)  
445 found that the nitrate concentration in the soil water taken beneath the rooting zone of  
446 matured artificial Japanese cedar plantations ( $607 \pm 59 \mu\text{M}$ ; 64-69 years old) was  
447 significantly higher than that of normal Japanese oak plantations ( $8.7 \pm 8.1 \mu\text{M}$ ; 24  
448 years old). Moreover, by adding ammonium nitrate ( $50 \text{ kg N ha}^{-1} \text{ year}^{-1}$ ) to the forest  
449 floor directly, Yang and Chiwa (2021) found that the nitrate concentration in the soil  
450 water of the matured artificial Japanese cedar plantations increased significantly faster  
451 than that of the normal Japanese oak plantations, probably because of the lower N  
452 uptake rates in the matured artificial Japanese cedar plantations. Because most of the  
453 artificial Japanese cedar/cypress plantations in the FK and MY catchments have reached  
454 their maturity ( $> 50$  years; Yang and Chiwa, 2021), the higher proportion of matured  
455 artificial Japanese cedar/cypress plantations in the FK1 catchment (Table 1) was highly  
456 responsible for the observed elevated leaching of nitrate, caused by the reduction in N  
457 uptake rates.

458 As a result, we concluded that the FK forested catchments were under the high  
459 nitrogen saturation stage, FK1 catchment especially, and the [high](#)-nitrogen saturation  
460 [stage-of-in](#) the FK1 catchments was responsible for the elevated  $M_{\text{total}}$ ,  $M_{\text{atm}}$ ,  $[\text{NO}_3^-]$ ,  
461  $[\text{NO}_3^-]_{\text{atm}}$  found in the stream eluted from the catchment (Figs. 3a, 3b, and 3c).

462  
463 4.3 The  $M_{\text{atm}}/D_{\text{atm}}$  ratio as an index of nitrogen saturation  
464 Past studies have used the concentration of stream nitrate as one of the important

465 indexes to evaluate the stage of nitrogen saturation in each forest (Aber, 1992; Huang  
466 et al., 2020; Rose et al., 2015; Stoddard, 1994). The strong linear relationship ( $R^2 =$   
467 0.7681;  $P < 0.0001$ ) between the stream nitrate concentration and the  $M_{atm}/D_{atm}$  ratio,  
468 except for the Qingyuan forested catchment (Fig. 3d), further supported that the  
469  $M_{atm}/D_{atm}$  ratio can be used as an alternative index of nitrogen saturation, as pointed out  
470 in Nakagawa et al. (2018).

471 The differences in the number of storm and/or snowmelt events could affect the  
472  $M_{atm}/D_{atm}$  ratio as well, because  $NO_3^-_{atm}$  could be injected into the stream water directly,  
473 along with the storm / snowmelt water (Tsunogai et al., 2014; Ding et al., 2022; Inamdar  
474 and Mitchell, 2006). In recent study, however, we found that the storm events have little  
475 impacts on the  $M_{atm}/D_{atm}$  ratio, based on monitoring temporal variation of  $[NO_3^-_{atm}]$  in  
476 a stream water during storm events (Ding et al., 2022). In addition, the low  $M_{atm}/D_{atm}$   
477 ratio found in Uryu forested catchment (0.7 %; Table 3) implied that the snowmelt has  
478 little impacts on the  $M_{atm}/D_{atm}$  ratio as well, because 30% of the annual mean  
479 precipitation was snow in Uryu forested catchment (Tsunogai et al., 2014).

480 The differences in the amount of precipitation, temperature, and the flux of stream  
481 water could affect the  $M_{atm}/D_{atm}$  ratio as well. As a result, the annual amount of  
482 precipitation, mean temperature, and the annual mean flux of stream water ( $F_{stream}$ ) in  
483 the forested catchments were compiled in Table S2. While the stream nitrate  
484 concentration showed the strong linear relationship ( $R^2 = 0.76$ ;  $P < 0.0001$ ) with the  
485  $M_{atm}/D_{atm}$  ratio (Fig. 3d), the precipitation, temperature, and  $F_{stream}$  did not show

486 significant relationship with the  $M_{atm}/D_{atm}$  ratio ( $P > 0.14$ ; Fig. 4). As a result, we  
487 concluded that the  $M_{atm}/D_{atm}$  ratio was mainly controlled by the progress of nitrogen  
488 saturation, rather than the differences in the number of storm and/or snowmelt events,  
489 the amount of precipitation, temperature, and the flux of stream water.

490 Moreover, ~~t~~The  $M_{atm}/D_{atm}$  ratio is a more reliable and robust index than the stream  
491 nitrate concentration, as explained below. The Qingyuan forested catchment can be  
492 classified into the highest nitrogen saturation stage based only on the highest stream  
493 nitrate concentration of 150  $\mu\text{M}$  (Table 3). However, based on the leaching flux of  
494 nitrogen via stream water monitored by Huang et al. (2020) for 4 years in the Qingyuan  
495 forested catchment, along with the deposition flux of nitrogen, we can obtain the  
496  $M_{atm}/D_{atm}$  ratio in the catchment to be a medium level of  $5.8 \pm 1.3 \%$ , implying that the  
497 nitrogen saturation stage was not ~~so very~~ high (Table 3). Huang et al. (2020) also  
498 concluded that the input of nitrogen exceeded the output in the catchment, and thus, the  
499 catchment was at stage 2 of nitrogen saturation. The  $M_{atm}/D_{atm}$  ratio in the Qingyuan  
500 forested catchment with a medium level among all forested catchments (Fig. 3d) should  
501 be a more reliable index of nitrogen saturation.

502 Compared with those in the other forested catchments in Table 3, the annual amount  
503 of precipitation (P) has the lowest value of 709 mm in the Qingyuan forested catchment.  
504 The flux of stream water ( $F_{stream}$ ) has the lowest value of 309 mm as well. Thus, we  
505 concluded that nitrate was relatively concentrated in the catchment because of the small  
506 precipitation, resulting in relative enrichment in the concentrations of both nitrate (150

507  $\mu\text{M}$ ) and unprocessed atmospheric nitrate (8.9  $\mu\text{M}$ ) in the stream.

508 While the concentration of stream nitrate, as an index of nitrogen saturation  
509 traditionally, can be influenced by the amount of precipitation, as demonstrated in the  
510 Qingyuan forested catchment, the  $M_{\text{atm}}/D_{\text{atm}}$  ratio is independent of the amount of  
511 precipitation (Fig. 4). Therefore, ~~we concluded that~~ the  $M_{\text{atm}}/D_{\text{atm}}$  ratio can be used as  
512 a more robust index for evaluating nitrogen saturation in each forested catchment.

513 The only concern on using the  $M_{\text{atm}}/D_{\text{atm}}$  ratio as the index of nitrogen saturation is  
514 the impact of the differences in the residence time of water in each catchment. The  
515 residence time of water varies from 1 month to more than 1 year in forested catchments  
516 (Asano et al., 2002; Farrick and Branfireun, 2015; Kabeya et al., 2008; Rodgers et al.,  
517 2005; Soulsby et al., 2006; Tetzlaff et al., 2007). The  $M_{\text{atm}}/D_{\text{atm}}$  ratio could be lower in  
518 catchments with longer residence time of water. We would like to clarify this in future  
519 studies by adding much more data of stream nitrate eluted from various forested  
520 catchments.

521

## 522 **5 Conclusions**

523 Both the concentrations and  $\Delta^{17}\text{O}$  of stream nitrate were determined for more than 2  
524 years in the forested catchments of FK (FK1 and FK2) and MY to determine the  
525  $M_{\text{atm}}/D_{\text{atm}}$  ratio for each catchment. The FK catchments exhibited higher  $M_{\text{atm}}/D_{\text{atm}}$  ratio  
526 than the MY catchment and other forested catchments reported in past studies, implying  
527 that the progress of nitrogen saturation in the FK catchments was severe. Both age and

528 proportion of artificial plantation in the FK catchments were responsible for the  
529 progress of nitrogen saturation. In addition, although past studies have commonly used  
530 the concentration of stream nitrate as an index to evaluate the progress of nitrogen  
531 saturation in forested catchments, it can be influenced by the amount of precipitation.

532 As a result, we concluded that the  $M_{atm}/D_{atm}$  ratio should be used as a more reliable  
533 index for evaluating the progress of nitrogen saturation because the  $M_{atm}/D_{atm}$  ratio is  
534 independent from the amount of precipitation.

535

536 *Data availability.* All the primary data are presented in the Supplement. The other data  
537 are available upon request to the corresponding author (Weitian Ding).

538

539 *Author contributions.* UT, FN, KS, and MC designed the study. MC and TK performed  
540 the field observations. WD, UT, and FN determined the concentrations and isotopic  
541 compositions of the samples. WD, TS, FN, and UT performed data analysis, and WD  
542 and UT wrote the paper with input from MC, TK, and KS.

543

544 *Competing interests.* The authors declare that they have no conflict of interest.

545

546 *Acknowledgements.*

547 We thank anonymous referees for valuable remarks on an earlier version of this  
548 paper. We also thank the Daisuke Nanki, Takuma Nakamura, and Yuko Muramatsu for

549 their long-term water sampling. Additionally, we are grateful to the members of the  
550 Biogeochemistry Group, Graduate School of Environmental Studies, Nagoya  
551 University, for their valuable support throughout this study. This work was supported  
552 by a Grant-in-Aid for Scientific Research from the Ministry of Education, Culture,  
553 Sports, Science, and Technology of Japan under grant numbers 22H00561, and  
554 17H00780, the Yanmar Environmental Sustainability Support Association, and the  
555 River fund of the river foundation, Japan. Weitian Ding would like to take this  
556 opportunity to thank the “Nagoya University Interdisciplinary Frontier Fellowship”  
557 supported by Nagoya University and JST, the establishment of university fellowships  
558 towards the creation of science technology innovation, Grant Number  
559 JPMJFS2120.~~would like to take this opportunity to thank the ‘Nagoya University~~  
560 ~~Interdisciplinary Frontier Fellowship’ supported by JST and Nagoya University.~~

561

## 562 **Reference**

563 Aber, J. D.: Nitrogen cycling and nitrogen saturation in temperate forest ecosystems,  
564 Trends Ecol. Evol., 7(7), 220–224, doi:10.1016/0169-5347(92)90048-G, 1992.  
565 Aber, J. D., Nadelhoffer, K. J., Steudler, P. and Melillo, J. M.: Nitrogen Saturation in  
566 Northern Forest Ecosystems, Bioscience, 39(6), 378–386, doi:10.2307/1311067,  
567 1989.  
568 Aikawa, M., Hiraki, T., Tamaki, M. and Shoga, M.: Difference between filtering-type  
569 bulk and wet-only data sets based on site classification, Atmos. Environ., 37(19),

570 2597–2603, doi:10.1016/S1352-2310(03)00214-0, 2003.

571 Alexander, B., Hastings, M. G., Allman, D. J., Dachs, J., Thornton, J. A. and

572 Kunasek, S. A.: Quantifying atmospheric nitrate formation pathways based on a

573 global model of the oxygen isotopic composition ( $\delta^{17}\text{O}$ ) of atmospheric nitrate,

574 *Atmos. Chem. Phys.*, 9(14), 5043–5056, doi:10.5194/acp-9-5043-2009, 2009.

575 [Asano, Y., Uchida, T. and Ohte, N.: Residence times and flow paths of water in steep](#)

576 [unchannelled catchments, Tanakami, Japan, J. Hydrol., 261\(1–4\), 173–192,](#)

577 [doi:10.1016/S0022-1694\(02\)00005-7, 2002.](#)

578 Environmental Laboratories Association of Japan: Acid Rain National Survey Report

579 2017, [https://tenbou.nies.go.jp/envgis\\_explain/acid\\_rain/content.html](https://tenbou.nies.go.jp/envgis_explain/acid_rain/content.html).

580 Bostic, J. T., Nelson, D. M., Sabo, R. D. and Eshleman, K. N.: Terrestrial Nitrogen

581 Inputs Affect the Export of Unprocessed Atmospheric Nitrate to Surface Waters:

582 Insights from Triple Oxygen Isotopes of Nitrate, *Ecosystems*, doi:10.1007/s10021-

583 021-00722-9, 2021.

584 Bourgeois, I., Savarino, J., Némery, J., Caillon, N., Albertin, S., Delbart, F., Voisin,

585 D. and Clément, J. C.: Atmospheric nitrate export in streams along a montane to

586 urban gradient, *Sci. Total Environ.*, 633, 329–340,

587 doi:10.1016/j.scitotenv.2018.03.141, 2018a.

588 Bourgeois, I., Savarino, J., Caillon, N., Angot, H., Barbero, A., Delbart, F., Voisin, D.

589 and Clément, J. C.: Tracing the Fate of Atmospheric Nitrate in a Subalpine Watershed

590 Using  $\Delta^{17}\text{O}$ , *Environ. Sci. Technol.*, 52(10), 5561–5570, doi:10.1021/acs.est.7b02395,

591 2018b.

592 Chiwa, M.: Ten-year determination of atmospheric phosphorus deposition at three  
593 forested sites in Japan, *Atmos. Environ.*, 223(May 2019), 1–7,  
594 doi:10.1016/j.atmosenv.2019.117247, 2020.

595 Chiwa, M.: Long-term changes in atmospheric nitrogen deposition and stream water  
596 nitrate leaching from forested watersheds in western Japan, *Environ. Pollut.*,  
597 287(November 2020), 117634, doi:10.1016/j.envpol.2021.117634, 2021.

598 Chiwa, M., Enoki, T., Higashi, N., Kumagai, T. and Otsuki, K.: The Increased  
599 Contribution of Atmospheric Nitrogen Deposition to Nitrogen Cycling in a Rural  
600 Forested Area of Kyushu, Japan, *Water, Air, Soil Pollut.*, 224(11), 1763,  
601 doi:10.1007/s11270-013-1763-2, 2013.

602 Chiwa, M., Onikura, N., Ide, J. and Kume, A.: Impact of N-Saturated Upland Forests  
603 on Downstream N Pollution in the Tatara River Basin, Japan, *Ecosystems*, 15(2),  
604 230–241, doi:10.1007/s10021-011-9505-z, 2012.

605 Chiwa, M.: Characteristics of atmospheric nitrogen and sulfur containing compounds  
606 in an inland suburban-forested site in northern Kyushu, western Japan, *Atmos. Res.*,  
607 96(4), 531–543, doi:10.1016/j.atmosres.2010.01.001, 2010.

608 Ding, W., Tsunogai, U., Nakagawa, F., Sambuichi, T., Sase, H., Morohashi, M., and  
609 Yotsuyanagi, H.: Tracing the source of nitrate in a forested stream showing elevated  
610 concentrations during storm events, *Biogeosciences*, 19, 3247–3261,  
611 <https://doi.org/10.5194/bg-19-3247-2022>, 2022.

- 612 Endo, T., Yagoh, H., Sato, K., Matsuda, K., Hayashi, K., Noguchi, I. and Sawada, K.:  
613 Regional characteristics of dry deposition of sulfur and nitrogen compounds at  
614 EANET sites in Japan from 2003 to 2008, *Atmos. Environ.*, 45(6), 1259–1267,  
615 doi:10.1016/j.atmosenv.2010.12.003, 2011.
- 616 [Farrick, K. K. and Branfireun, B. A.: Flowpaths, source water contributions and water](#)  
617 [residence times in a Mexican tropical dry forest catchment, \*J. Hydrol.\*, 529, 854–865,](#)  
618 [doi:10.1016/j.jhydrol.2015.08.059, 2015.](#)
- 619 [Kabeya, N., Shimizu, A., Nobuhiro, T. and Tamai, K.: Preliminary study of flow](#)  
620 [regimes and stream water residence times in multi-scale forested watersheds of central](#)  
621 [Cambodia, \*Paddy Water Environ.\*, 6\(1\), 25–35, doi:10.1007/s10333-008-0104-3,](#)  
622 [2008.](#)
- 623 Fukushima, K., Tateno, R. and Tokuchi, N.: Soil nitrogen dynamics during stand  
624 development after clear-cutting of Japanese cedar (*Cryptomeria japonica*) plantations,  
625 *J. For. Res.*, 16(5), 394–404, doi:10.1007/s10310-011-0286-1, 2011.
- 626 Galloway, J. N., Aber, J. D., Erisman, J. W., Seitzinger, S. P., Howarth, R. W.,  
627 Cowling, E. B. and Cosby, B. J.: The nitrogen cascade, *Bioscience*, 53(4), 341–356,  
628 doi:10.1641/0006-3568(2003)053[0341:TNC]2.0.CO;2, 2003.
- 629 Hattori, S., Nuñez Palma, Y., Itoh, Y., Kawasaki, M., Fujihara, Y., Takase, K. and  
630 Yoshida, N.: Isotopic evidence for seasonality of microbial internal nitrogen cycles in  
631 a temperate forested catchment with heavy snowfall, *Sci. Total Environ.*, 690, 290–  
632 299, doi:10.1016/j.scitotenv.2019.06.507, 2019.

633 Hirota, A., Tsunogai, U., Komatsu, D. D. and Nakagawa, F.: Simultaneous  
634 determination of  $\delta^{15}\text{N}$  and  $\delta^{18}\text{O}$  of  $\text{N}_2\text{O}$  and  $\delta^{13}\text{C}$  of  $\text{CH}_4$  in nanomolar quantities from  
635 a single water sample, *Rapid Commun. Mass Spectrom.*, 24, 1085–1092,  
636 doi:10.1002/rcm.4483, 2010.

637 Huang, S., Wang, F., Elliott, E. M., Zhu, F., Zhu, W., Koba, K., Yu, Z., Hobbie, E.  
638 A., Michalski, G., Kang, R., Wang, A., Zhu, J., Fu, S. and Fang, Y.: Multiyear  
639 Measurements on  $\Delta^{17}\text{O}$  of Stream Nitrate Indicate High Nitrate Production in a  
640 Temperate Forest, *Environ. Sci. Technol.*, 54(7), 4231–4239,  
641 doi:10.1021/acs.est.9b07839, 2020.

642 Inoue, T., Nakagawa, F., Shibata, H. and Tsunogai, U.: Vertical Changes in the Flux  
643 of Atmospheric Nitrate From a Forest Canopy to the Surface Soil Based on  $\Delta^{17}\text{O}$   
644 Values, *J. Geophys. Res. Biogeosciences*, 126(4), 1–18, doi:10.1029/2020JG005876,  
645 2021.

646 Inamdar, S. P. and Mitchell, M. J.: Hydrologic and topographic controls on storm-  
647 event exports of dissolved organic carbon (BOC) and nitrate across catchment scales,  
648 Water Resour. Res., 42(3), 1–16, doi:10.1029/2005WR004212, 2006.

649 Kaiser, J., Hastings, M. G., Houlton, B. Z., Röckmann, T. and Sigman, D. M.: Triple  
650 oxygen isotope analysis of nitrate using the denitrifier method and thermal  
651 decomposition of  $\text{N}_2\text{O}$ , *Anal. Chem.*, 79(2), 599–607, doi:10.1021/ac061022s, 2007.

652 Komatsu, D. D., Ishimura, T., Nakagawa, F. and Tsunogai, U.: Determination of the  
653  $^{15}\text{N}/^{14}\text{N}$ ,  $^{17}\text{O}/^{16}\text{O}$ , and  $^{18}\text{O}/^{16}\text{O}$  ratios of nitrous oxide by using continuous-flow

654 isotope-ratio mass spectrometry Daisuke, Rapid Commun. Mass Spectrom., 22, 1587–  
655 1596, doi:10.1002/rcm.3493, 2008a.

656 Komatsu, H., Maita, E. and Otsuki, K.: A model to estimate annual forest  
657 evapotranspiration in Japan from mean annual temperature, , 330–340,  
658 doi:10.1016/j.jhydrol.2007.10.006, 2008b.

659 Konno, U., Tsunogai, U., Komatsu, D. D., Daita, S., Nakagawa, F., Tsuda, A.,  
660 Matsui, T., Eum, Y. J. and Suzuki, K.: Determination of total N<sub>2</sub> fixation rates in the  
661 ocean taking into account both the particulate and filtrate fractions, Biogeosciences,  
662 7(8), 2369–2377, doi:10.5194/bg-7-2369-2010, 2010.

663 Matsuda, K.: Estimation of dry deposition for sulfur and nitrogen compounds in the  
664 atmosphere : Updated parameterization of deposition velocity, J. Japan Soc. Atmos.  
665 Environ., 43(6), 332–339, doi:10.11298/taiki1995.43.332, 2008.

666 McIlvin, M. R. and Altabet, M. A.: Chemical conversion of nitrate and nitrite to  
667 nitrous oxide for nitrogen and oxygen isotopic analysis in freshwater and seawater,  
668 Anal. Chem., 77(17), 5589–5595, doi:10.1021/ac050528s, 2005.

669 Michalski, G., Scott, Z., Kabiling, M. and Thiemens, M. H.: First measurements and  
670 modeling of  $\Delta^{17}\text{O}$  in atmospheric nitrate, Geophys. Res. Lett., 30(16), 3–6,  
671 doi:10.1029/2003GL017015, 2003.

672 Michalski, G., Meixner, T., Fenn, M., Hernandez, L., Sirulnik, A., Allen, E. and  
673 Thiemens, M.: Tracing Atmospheric Nitrate Deposition in a Complex Semiarid  
674 Ecosystem Using  $\Delta^{17}\text{O}$ , Environ. Sci. Technol., 38(7), 2175–2181,

675 doi:10.1021/es034980+, 2004.

676 Mitchell, M. J., Iwatsubo, G., Ohru, K. and Nakagawa, Y.: Nitrogen saturation in  
677 Japanese forests: An evaluation, *For. Ecol. Manage.*, 97(1), 39–51,

678 doi:10.1016/S0378-1127(97)00047-9, 1997.

679 Morin, S., Sander, R. and Savarino, J.: Simulation of the diurnal variations of the  
680 oxygen isotope anomaly ( $\Delta^{17}\text{O}$ ) of reactive atmospheric species, *Atmos. Chem. Phys.*,  
681 11(8), 3653–3671, doi:10.5194/acp-11-3653-2011, 2011.

682 Nakagawa, F., Suzuki, A., Daita, S., Ohyama, T., Komatsu, D. D. and Tsunogai, U.:  
683 Tracing atmospheric nitrate in groundwater using triple oxygen isotopes: Evaluation  
684 based on bottled drinking water, *Biogeosciences*, 10(6), 3547–3558, doi:10.5194/bg-  
685 10-3547-2013, 2013.

686 Nakagawa, F., Tsunogai, U., Obata, Y., Ando, K., Yamashita, N., Saito, T.,  
687 Uchiyama, S., Morohashi, M. and Sase, H.: Export flux of unprocessed atmospheric  
688 nitrate from temperate forested catchments: A possible new index for nitrogen  
689 saturation, *Biogeosciences*, 15(22), 7025–7042, doi:10.5194/bg-15-7025-2018, 2018.

690 Nelson, D. M., Tsunogai, U., Ding, D., Ohyama, T., Komatsu, D. D., Nakagawa, F.,  
691 Noguchi, I. and Yamaguchi, T.: Triple oxygen isotopes indicate urbanization affects  
692 sources of nitrate in wet and dry atmospheric deposition, *Atmos. Chem. Phys.*, 18(9),  
693 6381–6392, doi:10.5194/acp-18-6381-2018, 2018.

694 Ohru, K. and Mitchell, M. J.: Nitrogen Saturation in Japanese Forested Watersheds  
695 Author ( s ): Kiyokazu Ohru and Myron J . Mitchell Published by : Wiley Stable

696 URL : <http://www.jstor.org/stable/2269507> Accessed : 05-07-2016 04 : 51 UTC Your  
697 use of the JSTOR archive indicates your ac, , 7(2), 391–401, 1997.

698 Paerl, H. W. and Huisman, J.: Climate change: A catalyst for global expansion of  
699 harmful cyanobacterial blooms, *Environ. Microbiol. Rep.*, 1(1), 27–37,  
700 doi:10.1111/j.1758-2229.2008.00004.x, 2009.

701 Peterjohn, W. T., Adams, M. B. and Gilliam, F. S.: Symptoms of nitrogen saturation  
702 in two central Appalachian hardwood forest ecosystems, *Biogeochemistry*, 35(3),  
703 507–522, doi:10.1007/BF02183038, 1996.

704 Riha, K. M., Michalski, G., Gallo, E. L., Lohse, K. A., Brooks, P. D. and Meixner, T.:  
705 High Atmospheric Nitrate Inputs and Nitrogen Turnover in Semi-arid Urban  
706 Catchments, *Ecosystems*, 17(8), 1309–1325, doi:10.1007/s10021-014-9797-x, 2014.

707 Rodgers, P., Soulsby, C., Waldron, S. and Tetzlaff, D.: Using stable isotope tracers to  
708 identify hydrological flow paths, residence times and landscape controls in a  
709 mesoscale catchment, *Hydrol. Earth Syst. Sci. Discuss.*, 9, 139–155, 2005.

710 Rose, L. A., Elliott, E. M. and Adams, M. B.: Triple Nitrate Isotopes Indicate  
711 Differing Nitrate Source Contributions to Streams Across a Nitrogen Saturation  
712 Gradient, *Ecosystems*, 18(7), 1209–1223, doi:10.1007/s10021-015-9891-8, 2015.

713 Sabo, R. D., Nelson, D. M. and Eshleman, K. N.: Episodic, seasonal, and annual  
714 export of atmospheric and microbial nitrate from a temperate forest, *Geophys. Res.*  
715 Lett.

716 , 43(2), 683–691, doi:10.1002/2015GL066758, 2016.  
Sappa, G., Ferranti, F. and Pecchia, G. M.: Validation Of Salt Dilution Method For

717 [Discharge Measurements In The Upper Valley Of Aniene River \(Central Italy\), Recent](#)  
718 [Adv. Environ. Ecosyst. Dev., \(October 2015\), 42–48, 2015.](#)  
719 [Soulsby, C., Tetzlaff, D., Rodgers, P., Dunn, S. and Waldron, S.: Runoff processes,](#)  
720 [stream water residence times and controlling landscape characteristics in a mesoscale](#)  
721 [catchment: An initial evaluation, J. Hydrol., 325\(1–4\), 197–221,](#)  
722 [doi:10.1016/j.jhydrol.2005.10.024, 2006.](#)

723 Stoddard, J. L.: Long-Term Changes in Watershed Retention of Nitrogen, , 223–284,  
724 doi:10.1021/ba-1994-0237.ch008, 1994.

725 [Tetzlaff, D., Malcolm, I. A. and Soulsby, C.: Influence of forestry, environmental](#)  
726 [change and climatic variability on the hydrology, hydrochemistry and residence times](#)  
727 [of upland catchments, J. Hydrol., 346\(3–4\), 93–111,](#)  
728 [doi:10.1016/j.jhydrol.2007.08.016, 2007.](#)

729 Tsunogai, U., Komatsu, D. D., Daita, S., Kazemi, G. A., Nakagawa, F., Noguchi, I.  
730 and Zhang, J.: Tracing the fate of atmospheric nitrate deposited onto a forest  
731 ecosystem in Eastern Asia using  $\Delta^{17}\text{O}$ , Atmos. Chem. Phys., 10(4), 1809–1820,  
732 doi:10.5194/acp-10-1809-2010, 2010.

733 Tsunogai, U., Daita, S., Komatsu, D. D., Nakagawa, F. and Tanaka, A.: Quantifying  
734 nitrate dynamics in an oligotrophic lake using  $\Delta^{17}\text{O}$ , Biogeosciences, 8(3), 687–702,  
735 doi:10.5194/bg-8-687-2011, 2011.

736 Tsunogai, U., Komatsu, D. D., Ohyama, T., Suzuki, A., Nakagawa, F., Noguchi, I.,  
737 Takagi, K. and Nomura, M.: Quantifying the effects of clear-cutting and strip-cutting

738 on nitrate dynamics in a forested watershed using triple oxygen isotopes as tracers, ,  
739 (1), 5411–5424, doi:10.5194/bg-11-5411-2014, 2014.

740 Tsunogai, U., Miyauchi, T., Ohyama, T., Komatsu, D. D., Nakagawa, F., Obata, Y.,  
741 Sato, K. and Ohizumi, T.: Accurate and precise quantification of atmospheric nitrate  
742 in streams draining land of various uses by using triple oxygen isotopes as tracers,  
743 Biogeosciences, 13(11), 3441–3459, doi:10.5194/bg-13-3441-2016, 2016.

744 Tsunogai, U., Miyauchi, T., Ohyama, T., Komatsu, D. D., Ito, M. and Nakagawa, F.:  
745 Quantifying nitrate dynamics in a mesotrophic lake using triple oxygen isotopes as  
746 tracers, Limnol. Oceanogr., 63, S458–S476, doi:10.1002/lno.10775, 2018.

747 Vitousek, P. M. and Howarth, R. W.: Nitrogen limitation on land and in the sea: How  
748 can it occur?, Biogeochemistry, 13(2), 87–115, doi:10.1007/BF00002772, 1991.

749 Watanabe, M., Miura, S., Hasegawa, S., Koshikawa, M. K., Takamatsu, T., Kohzu,  
750 A., Imai, A. and Hayashi, S.: Coniferous coverage as well as catchment steepness  
751 influences local stream nitrate concentrations within a nitrogen-saturated forest in  
752 central Japan, Sci. Total Environ., 636, 539–546, doi:10.1016/j.scitotenv.2018.04.307,  
753 2018.

754 Yamazaki, A., Watanabe, T. and Tsunogai, U.: Nitrogen isotopes of organic nitrogen  
755 in reef coral skeletons as a proxy of tropical nutrient dynamics, Geophys. Res. Lett.,  
756 38(19), 1–5, doi:10.1029/2011GL049053, 2011.

757 Yang, R. and Chiwa, M.: Low nitrogen retention in a Japanese cedar plantation in a  
758 suburban area, western Japan, Sci. Rep., 11(1), 1–7, doi:10.1038/s41598-021-84753-

759 1, 2021.

760 **Table 1.** Plant information for each forested catchment (Chiwa, 2021).

Overstory vegetation (%)	FK1	FK2	MY
Artificial Japanese cedar/cypress plantation	74	40	16
Other artificial coniferous plantations	<1	<1	7
Natural trees	10	54	75
Others	16	5	2

761

762

763

764 **Table 2.** Average concentrations of stream nitrate ( $[\text{NO}_3^-]_{\text{avg}}$ ), the average  
765 concentrations of unprocessed  $\text{NO}_3^-_{\text{atm}}$  in streams ( $[\text{NO}_3^-_{\text{atm}}]_{\text{avg}}$ ), the annual export flux  
766 of  $\text{NO}_3^-$  per unit area of catchments ( $M_{\text{total}}$ ), the annual export flux of  $\text{NO}_3^-_{\text{atm}}$  per unit  
767 area of catchments ( $M_{\text{atm}}$ ), the deposition flux of  $\text{NO}_3^-_{\text{atm}}$  per unit area of catchment  
768 ( $D_{\text{atm}}$ ), and the  $M_{\text{atm}}/D_{\text{atm}}$  ratios in the study catchments.

	FK1	FK2	MY
$[\text{NO}_3^-]_{\text{avg}}$ ( $\mu\text{M}$ )	109.5	<u>90.9</u> <u>94.2</u>	7.3
$[\text{NO}_3^-_{\text{atm}}]_{\text{avg}}$ ( $\mu\text{M}$ )	$10.80 \pm 1.65$	<u>6.09</u> <u>5.06</u> $\pm$ <u>0.92</u> <u>1.05</u>	$0.16 \pm 0.05$
$M_{\text{total}}$ ( $\text{mmol m}^{-2} \text{yr}^{-1}$ )	<u>98.8</u> <u>97.9</u> $\pm$ 17.8	<u>82.0</u> <u>84.2</u> $\pm$ <u>14.8</u> <u>15.3</u>	<u>23.7</u> <u>22.6</u> $\pm$ 1.2
$M_{\text{atm}}$ ( $\text{mmol m}^{-2} \text{yr}^{-1}$ )	$9.7 \pm 2.3$	<u>4.6</u> <u>5.4</u> $\pm$ <u>1.2</u> <u>1.4</u>	$0.5 \pm 0.2$ <u>1</u>
$D_{\text{atm}}$ ( $\text{mmol m}^{-2} \text{yr}^{-1}$ )	$69.3 \pm 13.9$	$69.3 \pm 13.9$	$40.1 \pm 8.0$
$M_{\text{atm}}/D_{\text{atm}}$ (%)	<u>14.1</u> <u>13.9</u> $\pm$ <u>4.4</u> <u>3</u>	<u>6.6</u> <u>7.9</u> $\pm$ <u>2.1</u> <u>2.5</u>	<u>1.3</u> <u>2</u> $\pm$ <u>0.5</u> <u>4</u>

769

770

771

772

773 **Table 3.** The annual amount of precipitation (P), the average concentration of stream  
 774 nitrate ( $[\text{NO}_3^-]_{\text{avg}}$ ), the nitrogen saturation stage, the average concentration of  
 775 unprocessed  $\text{NO}_3^-_{\text{atm}}$  in streams ( $[\text{NO}_3^-_{\text{atm}}]_{\text{avg}}$ ), the annual export flux of  $\text{NO}_3^-$  per unit  
 776 area of catchment ( $M_{\text{total}}$ ), the annual export flux of  $\text{NO}_3^-_{\text{atm}}$  per unit area of catchment  
 777 ( $M_{\text{atm}}$ ), the deposition flux of  $\text{NO}_3^-_{\text{atm}}$  per unit area of catchment ( $D_{\text{atm}}$ ), and the  
 778  $M_{\text{atm}}/D_{\text{atm}}$  ratio in the FK1, FK2, and MY, along with those in the catchments studied in  
 779 past studies using  $\Delta^{17}\text{O}$  of nitrate as a tracer.

	P mm	$[\text{NO}_3^-]_{\text{avg}}$ $\mu\text{M}$	N stage <sup>*</sup>	$[\text{NO}_3^-_{\text{atm}}]_{\text{avg}}$ $\mu\text{M}$	$M_{\text{atm}}$ $\text{mmol m}^{-2} \text{yr}^{-1}$	$M_{\text{total}}$ $\text{mmol m}^{-2} \text{yr}^{-1}$	$D_{\text{atm}}$	$M_{\text{atm}}/D_{\text{atm}}$ %
FK1 <sup>a</sup>	1777 <sup>1769</sup>	109.5	-	10.8	9.7	98.8 <sup>97.9</sup>	69.3	14.1 <sup>13.9</sup>
FK2 <sup>a</sup>	1777 <sup>1769</sup>	90.9 <sup>94.2</sup>	-	5.06 <sup>6.1</sup>	4.6 <sup>5.4</sup>	82.0 <sup>84.2</sup>	69.3	6.6 <sup>7.9</sup>
MY <sup>a</sup>	3981 <sup>3837</sup>	7.3	-	0.2	0.5	23.7 <sup>22.6</sup>	40.1	1.3 <sup>2</sup>
KJ <sup>b</sup>	2500	58.4	-	3.3	4.3	76.4	45.6	9.4
IJ1 <sup>b</sup>	3300	24.4	2	1.4	2.9	50.1	44.5	6.5
IJ2 <sup>b</sup>	3300	17.1	-	0.6	1.2	35.1	44.5	2.6
Fernow1 <sup>c</sup>	1450	17.9	1	1.6	0.8	9.3	23.4	3.6
Fernow2 <sup>c</sup>	1450	34.3	2	3.4	1.5	14.8	23.4	6.3
Fernow3 <sup>c</sup>	1450	60.0	3	4.2	2.4	34.5	23.4	10.3
Uryu <sup>d</sup>	1170	0.7	-	0.1	0.1	1.0	18.6	0.7
Qingyuan <sup>e</sup>	709	150.0	2	8.9	2.9	49.3	50.0	5.8

780 a: This study

781 b: Nakagawa et al., 2018; Nakahara et al., 2010

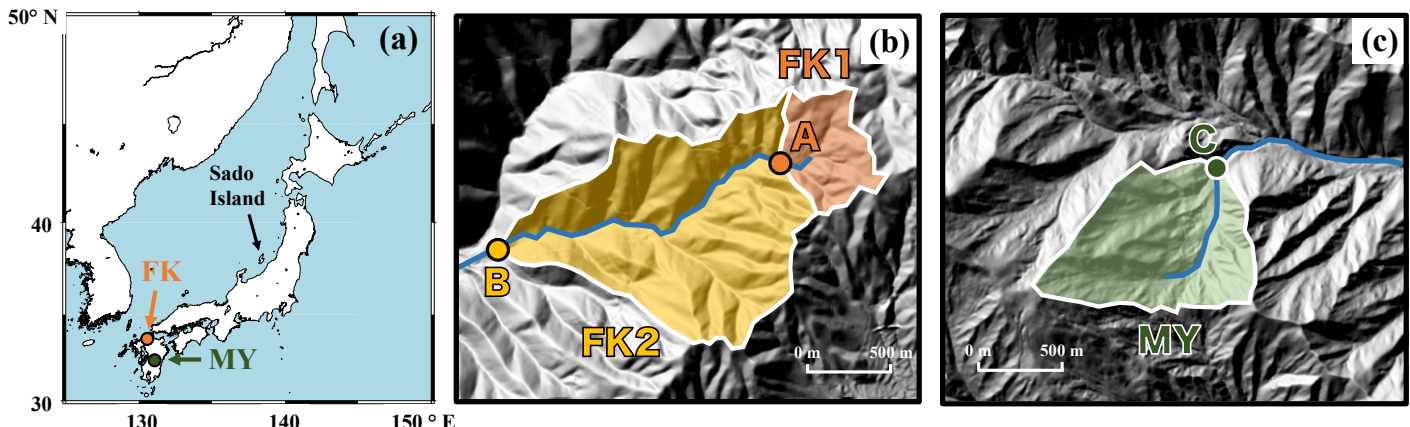
782 c: Rose et al., 2015

783 d: Tsunogai et al., 2014

784 e: Huang et al., 2020

785 \*: N saturation stage estimated in past studies

786 -: No data



787 **Figure 1.** A map showing the locations of the study [catchments](#)[watersheds](#) (FK and  
 788 MY) in Japan (a), and the maps of FK1, FK2 (b) and MY catchments (c), [shown by](#)  
 789 [orange, yellow, and green areas, respectively](#), together with the sampling [point](#)[station](#)  
 790 [A, B, and C, respectively](#), shown by orange, yellow, and green circles, respectively.

791

792

793

794

795

796

797

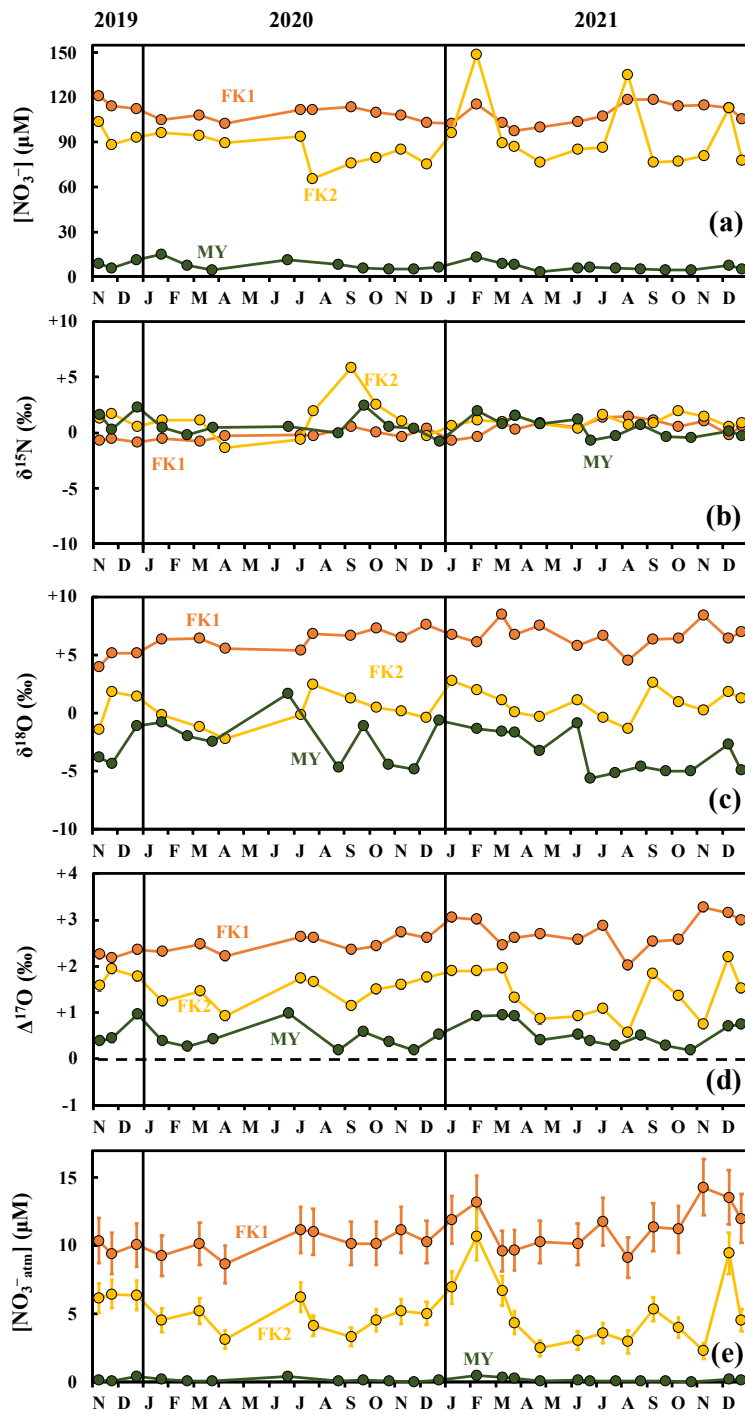
798

799

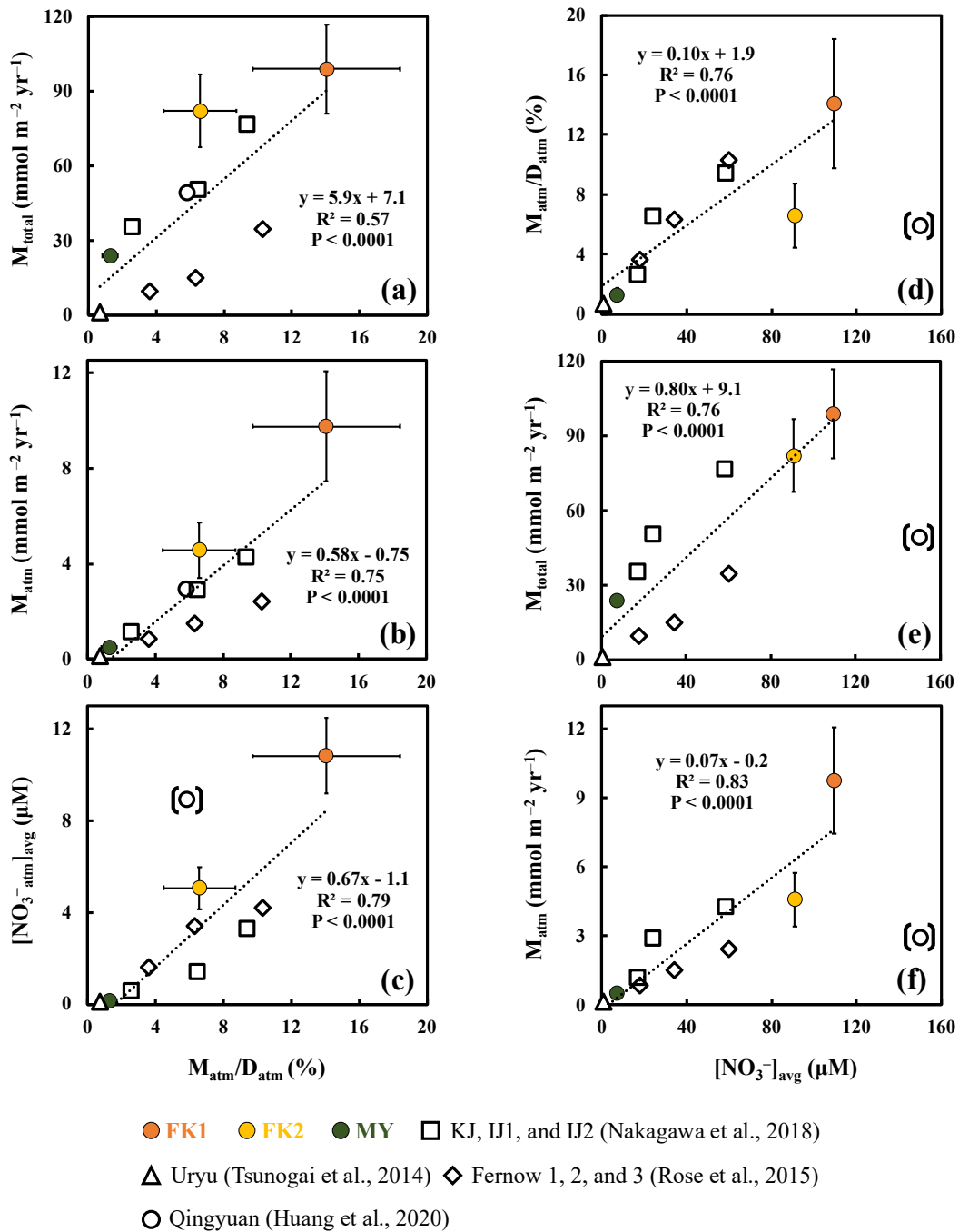
800

801

802



803 **Figure 2.** Temporal variations in concentrations of stream nitrate (FK1: orange circles;  
804 FK2: yellow circles; MY: green circles) (a), together with those in  $\delta^{15}\text{N}$  (b),  $\delta^{18}\text{O}$  (c),  
805 and  $\Delta^{17}\text{O}$  (d) of nitrate, and the concentration of unprocessed  $\text{NO}_3^-_{\text{atm}}$  ( $[\text{NO}_3^-_{\text{atm}}]$ ) (e) in  
806 the stream water of the FK1, FK2, and MY forested catchments. Error bars smaller than  
807 the sizes of the symbols are not presented.



808 **Figure 3.** Annual export flux of nitrate per unit area ( $M_{\text{total}}$ ) plotted as a function of the  
809  $M_{\text{atm}}/\text{D}_{\text{atm}}$  ratio in each forested catchment (a); the annual export flux of unprocessed  
810 atmospheric nitrate per unit area ( $M_{\text{atm}}$ ) plotted as a function of the  $M_{\text{atm}}/\text{D}_{\text{atm}}$  ratio (b);  
811 the average concentration of  $\text{NO}_3^-_{\text{atm}}$  ( $[\text{NO}_3^-_{\text{atm}}]_{\text{avg}}$ ) plotted as a function of the  
812  $M_{\text{atm}}/\text{D}_{\text{atm}}$  ratio (c); the  $M_{\text{atm}}/\text{D}_{\text{atm}}$  ratio plotted as a function of the average concentration

813 of nitrate ( $[\text{NO}_3^-]_{\text{avg}}$ ) (d); the  $M_{\text{total}}$  plotted as a function of  $[\text{NO}_3^-]_{\text{avg}}$  (e); the  $M_{\text{atm}}$   
814 plotted as a function of  $[\text{NO}_3^-]_{\text{avg}}$  (f) (FK1: orange circles; FK2: yellow circles; MY:  
815 green circles). Those determined for the forested catchments in past studies are plotted  
816 as well (Qingyuan: white circle (Huang et al., 2020); KJ, IJ1, and IJ2: white squares  
817 (Nakagawa et al., 2018); Fernow 1, 2, and 3: white diamonds (Lucy et al., 2015); Uryu:  
818 white triangle (Tsunogai., 2014)). The data obtained in the Qingyuan forested  
819 catchment are shown in parentheses and excluded from the calculation to estimate  
820 correlation coefficients (see text for the reason).

821

822

823

824

825

826

827

828

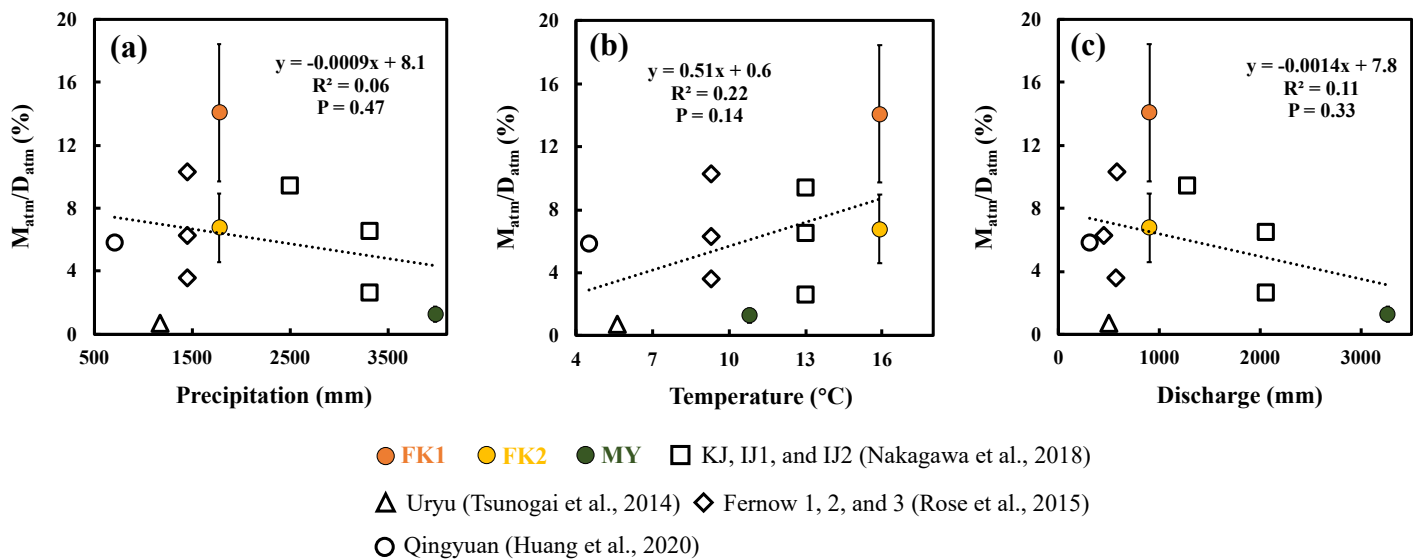
829

830

831

832

833

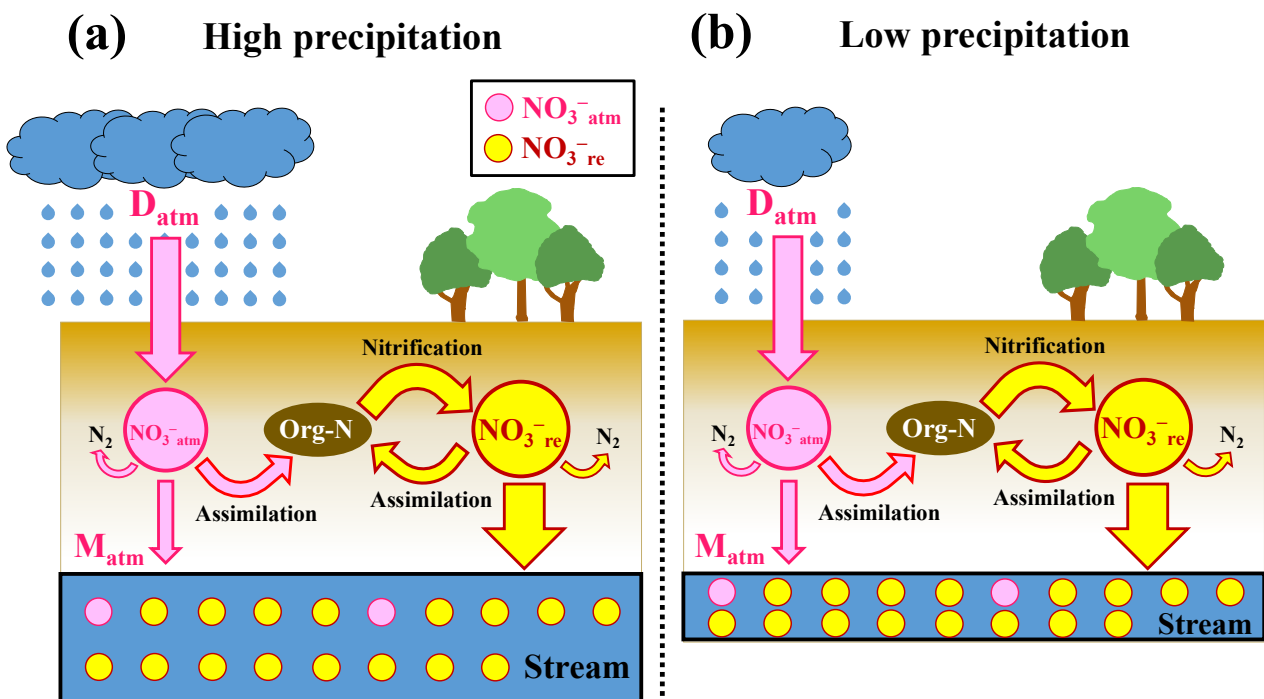


834 **Figure 4.** the  $M_{atm}/D_{atm}$  ratio plotted as a function of the amount of precipitation (a),  
835 the  $M_{atm}/D_{atm}$  ratio plotted as a function of the temperature (b), and the  $M_{atm}/D_{atm}$  ratio  
836 plotted as a function of flux of stream water (c) (FK1: orange circles; FK2: yellow  
837 circles; MY: green circles). Those determined for the forested catchments in past studies  
838 are plotted as well.

839

840

841



842 **Figure 54.** Schematic diagram showing the biogeochemical processing of nitrate in  
 843 forested catchments under high precipitation (a) and low precipitation (b), where  
 844  $\text{NO}_3^-_{\text{atm}}$  (unprocessed atmospheric nitrate) is represented by pink circles,  $\text{NO}_3^-_{\text{re}}$  by  
 845 yellow circles, the flows of  $\text{NO}_3^-_{\text{atm}}$  by pink arrows, and those of  $\text{NO}_3^-_{\text{re}}$  (remineralized  
 846 nitrate) by yellow arrows (modified after Nakagawa., 2018). Although the deposition  
 847 rates of  $\text{NO}_3^-_{\text{atm}}$  ( $D_{\text{atm}}$ ) and the biogeochemical reaction rates between (a) and (b) are  
 848 the same, we can expect high  $[\text{NO}_3^-]$  in (b). On the other hand, the  $M_{\text{atm}}/D_{\text{atm}}$  ratio  
 849 between (a) and (b) are the same.